Nonlinear Degradation Analysis of Arch-Dam Blocks by using Deterministic and Probabilistic Seismic Input

Enrico Zacchei[1], José Luis Molina[1] and Reyolando M. L. R. F. Brasil[2]
[1]Higher Polytechnic School of Ávila, University of Salamanca (USAL), 50 Hornos Caleros, Spain
enricozacchei@usal.es
[2]Polytechnic School of São Paulo, University of São Paulo (USP), 380 Prof. Luciano Gualberto, Brazil

Abstract

This paper aims to define the non-linear response of arch-dam blocks. The plastic-degradation theory has been used to define the reduction of the elasto-plastic modulus during the hysteretic cycles. The parameters that are used to apply the model are obtained by literature and numerical analysis. In this sense, working with a reduction of the elasto-plastic modulus is useful to define the displacement of the structure. The seismic input has been obtained from probabilistic and deterministic seismic hazard analyses. For that, a series of several earthquakes have been chosen to perform the time-history analysis. The response of the structure blocks under four earthquakes has been made by using a step-by-step direct integration. An application to Rules Dam has been made to test the method.

1 Introduction

Due to an increasing demand for power and drinkable water, dams continue to be important structures for the population. The use of the impounding reservoir of the Rules Dam is for water storage, protection from floods and irrigation. In literature there are several case studies about seismic dams but only few of them are about arch dams which have suffered serious damage under intensive earthquake[1]. Consequently, there is not much scientific knowledge on types of cracking. In recent years, the nonlinear dynamic response of dams under earthquake actions, including cracking of the concrete, has attracted more researchers[1,2,3]. Some significant topics are, for example, the appropriate damping ratio for the concrete[4].

This paper is divided into three parts: definition of the seismic input where the dam is placed, definition of the hypothesis of the model, and analysis of the non-linear response. Definition of the seismic input is important because dams in southern Spain suffer from moderate to high earthquakes. The study of the model hypothesis is necessary for not under- or over-estimating the stresses, neglecting water compressibility, wave absorption at the reservoir boundary and foundation mass and damping.

The response of the structure blocks under four seisms was made by a non-linear seismic analysis using a step-by-step integration. Under cyclic loading, the mechanism of the stiffness degradation is difficult to define due to the formation of micro-cracks. Internal damage of structures inevitably lead to change of the structural dynamic parameters; as, for example, natural frequency, damping and vibration shapes. The softening and losing of the strength (compression and tension), in the broken regions under axial cyclic loadings, affect the seismic safety of the arch dam. The horizontal tensile stress, for example, produces cracks because the concrete tensile capacity is weak.

To carry out the non-linear analysis, the plasticity model has been used because it is rather simple to develop compared, for example, to the fracture mechanic model[5]. The former model defines the elastic-plastic modulus, whereas the latter defines the potential crack that depends on the softening curve, which is rather difficult to calculate.

A Finite Element Analysis (FEA) has also been carried out for an easy computation of the stresses of arch-dams. In 2-D analysis it is possible to consider a dam block as an equivalent simple oscillator because, during the motion, the mass is the most predominant parameter[6]. These approximations are generally useful for having a reference about the results because it is difficult to calculate satisfactorily the dam body's stress results and its foundation.

Finally, in 3-D analysis the interaction between the block vertical joints, dam-foundation and dam-water can be analysed. The spatial variations of the ground motion are not ignored. A strong intensity of the seism can produce damage to the entire structure or only to some parts of it. The damage mechanism can occur in the neck as well as, in the separation line between foundation and dam, in the singular points (heel and toe), in the vertical joints and discontinuity slopes. This mechanism is caused by several factors such as deflection of the crest, overturning, sliding and loss of the passive resistance of the rocky wedge.

2 Seismic Input

The seismic input has been obtained here from Probabilistic and Deterministic Seismic Hazard Analyses (P- and D-SHA)[7]. The P- and the D-SHA obtain the most probable occurrence of earthquakes and the most intense ones. The PSHA is calculated using Cornell method and it is developed in four steps: (i) identification and characterization of earthquake sources (http://info.igme.es/zesis/); (ii) characterization of the magnitude-recurrence distributions with the hypothesis of the Poisson process, which implies the Gutenberg and Richter law; (iii) evaluation of the ground motion where the Rules Dam is placed using attenuation equations[8,9]; and (iv) calculation of the hazard curves. The DSHA is developed in three steps: (i) selection of the historic earthquake, (ii) evaluation of the ground motion where the Rules Dam is placed using attenuation equations[8,10]; and (iii) calculation of spectra accelerations.

Both analyses are based on stochastic processes related to the standard deviation (margin of error), which is present in the attenuation equations. In the PSHA the standard deviation is equal to zero. Instead, in the DSHA, since it does not take into account the probability of occurrence (return period), it is convenient to consider the standard deviations – the standard deviation values used here are ± 0.26 for SP96 and ± 0.32 for Am96.

The historic earthquake chosen to be used for the DSHA is the event numbered 2877, which occurred in Spain on July 16th, 1910, having as its magnitude moment M_w 6.1 (= surface wave magnitude M_s 6.0) and its site-station epicentral distance of 6.82 km (http://www.ign.es).

This specific seismic analyses results help to choose a series of records with several different levels of intensity which are useful to carry out the nonlinear dynamic analysis of the structure. Four records have been chosen, i.e. Greece, 13/09/1986 (event name: GR-1986-0006); Italy, 26/09/1997 (event name: IT-1997-0006); Italy, 29/05/2012 (event name: IT-2010-0011) and Turkey, 1999 (TK-1999-0415) (esm.mi.ingv.it).

Figure 1 shows Pseudo Spectra Acceleration (PSA) obtained by probabilistic analysis and for the deterministic analysis, and the Turkey 1999 record. Table 1 shows some relevant values. The subscripts refer to the used attenuation equations, i.e. SP96[8], Am96[9] and Am05[10]. These values are in accordance to similar studies in literature[11,12].

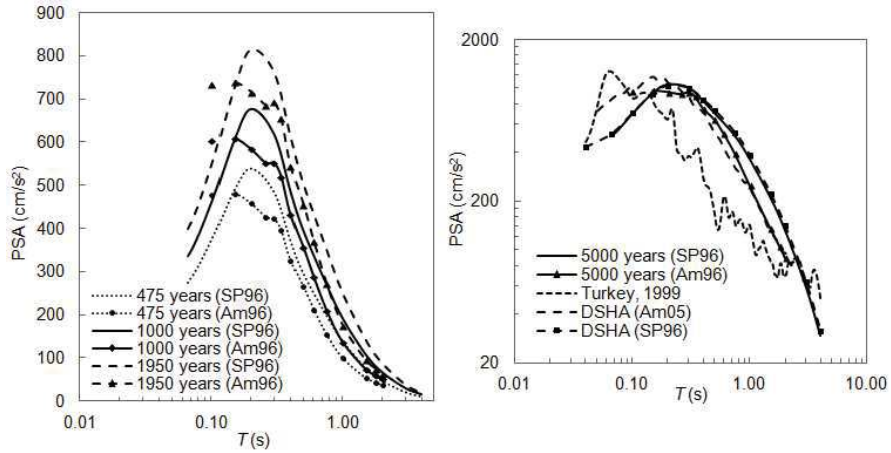

Fig. 1 PSA for different return periods (left and right), deterministic spectra (right) and Turkey 1999 record (right).

Table 1 Some results of the probabilistic and deterministic analysis.

		475 years	1000 years	1950 years	5000 years	-
PSHA*	$PSA\|_{SP96}$ [cm/s^2]	463.63	593.10	729.17	962.37	-
	$PSA\|_{Am96}$ [cm/s^2]	406.52	527.20	659.06	884.02	-
DSHA**	$PSA\|_{SP96}$ [cm/s^2]	-	-	-	-	1038.32
	$PSA\|_{Am05}$ [cm/s^2]	-	-	-	-	1165.84

*These PSA numbers are mean values of the structural period (T) 0.20–0.40 s (dam and system periods as well as the maximum PSA, which have been obtained in the analysis, are included in this interval).
**The $DSHA|_{Am05}$ is calculated for $T = 0.15$ s whereas the $DSHA|_{SP96}$ for $T = 0.2$ s.

3 Structural Data of the Model

Rules Dam is a concrete arch-gravity structure, situated in southern Spain in the Granada province. Table 2 shows data of the structure and reservoir.

Table 2 Data of the Rules Dam and the reservoir.

Crown length [m]	620.0
Radius [m]	500.0
Curvature angle in plan [°]	71.04
Bottom elevation of the higher vertical cantilever [m]	119.67
Top elevation of the higher vertical cantilever [m]	250.00
Mean higher of cantilevers [m]	74.783
Capacity of the reservoir for the maximum operating level [Hm^3]	117.07
Area of the reservoir for the maximum operating level [Ha]	308.0
Area of the water basin [km^2]	1070.0

Figure 2 shows the studied five blocks (in dark gray) (from the left to the right: 14A, 12A, 10A, 8A, 0A), the contact joints between blocks and the mode governing equations of the dam-foundation-water system (1), (2) and (3) that will be detailed below. The used coordinate references in the equations are: the *x*-axis is parallel to the flow direction and the Down-Stream (DS) direction is positive; the *y*-axis is parallel to the dam height direction and the upward is positive; the *z*-axis is perpendicular to the flow direction.

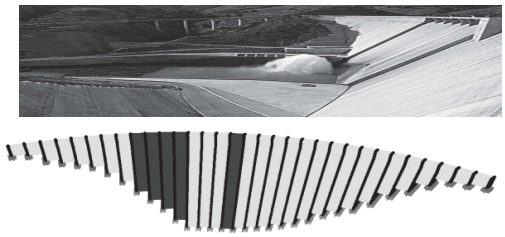

$$\frac{\partial \Pi}{\partial n}(\hat{n},t) + \rho_w \ddot{v}_g^n(t) + \rho_w \varphi_1^n(\hat{n})\ddot{X}_1^n(t) = 0 \quad (1)$$

$$\frac{\partial \Pi}{\partial n}(\hat{n},t) + \rho_w \ddot{v}_g^n(t) - \mu(\alpha_w, \tilde{v}_{b,w})\frac{\partial \Pi}{\partial t}(\hat{n},t) = 0 \quad (2)$$

$$\frac{\partial \Pi}{\partial n}(\hat{n},t) + \frac{1}{\tilde{v}_{b,w}}\frac{\partial \Pi}{\partial t}(\hat{n},t) = 0 \quad (3)$$

Fig. 2 Rules Dam DS photo (above), and (below) dam blocks, contact joint between blocks and foundation springs.

Table 3 shows data of the FEA of the dam (the SAP2000 software has been used for the modelling) and Table 4 shows data of the studied blocks.

Table 3 Data of FEA of the dam.

Number dam blocks	32
Number blocks of the central spillway	7
Mass density of the concrete [kN/m^3]*	20.64
Number of the solid elements (s_i)	32980
Number of the joints (j_i)	36925
j_i/s_i	1.119
Number of restraints defined (k^n_f)	3465
Number of angular divisions (Δz_i)	207
Number of radial divisions (Δx_i)	33.8
Number of vertical divisions (Δy_i)	47.4

*Considering the voids, the mass density of the concrete is 14% of 24 kN/m^3.

Arch-dams resists to the external forces thanks to the combination of the arches (horizontal elements) and the cantilevers (vertical elements). The interaction between arch and cantilever units is continuing: the load actions create movements that consist of *n* translational and *n* rotational components. Vertical *y* movements and rotations in vertical *y* planes might be negligible. The foundation has been considered rocky and mass-less. Mass-less foundation model takes into account only the elastic stiffness of the foundation medium, whereas the inertia and damping effects are neglected. Assuming the rigid foundation the stresses decrease because the soil rock model does not take into account the effects of the foundation: $k^n_f \rightarrow \infty$. The order of the magnitude of the rocky foundation stiffness is 10^9 kN/m, and for the mass-less foundation stiffness is 10^6 kN/m. Using the latter stiffness value the vertical stress due to the dam dead-weight increases 1.476 times (with $k^n_f = 0$ the vertical stresses are 147.69 times higher). The thrusts against the dam of the cross-canyon (abutments) excitation are been neglected since the behaviour is quasi-symmetrical.

Table 4 Data of the studied blocks.

Block	Elevation [m]	Height [m]	Base* [m]	Width [m]	Volume [m^3]	Mass [10^6 kg]	Equivalent Period [s]	Equivalent Inertia [m^4]
14A	172.43	77.58	60.51	19.51	45784.76	109.883	0.193	24148.874
12A	158.54	91.46	71.34	19.51	63638.62	152.733	0.228	39572.786
10A	144.62	105.38	82.20	19.51	84487.75	202.771	0.262	60534.939
8A	128.82	121.18	94.52	19.51	111729.52	268.151	0.302	92059.239
0A	119.67	130.33	101.66	18.90	125203.13	300.488	0.324	110946.542

*The base is calculated considering a triangular dam shape with DS and Up-Stream (US) slope faces of 1:0.60 and 1:0.18, respectively.

4 Hypotheses of the Model

The hydraulic hypothesis[13,14] of the two- and three-dimensional (*x,y,z*) analyses are shown in this section. The system – governed by second order differential equations – is composed by the concrete dam, which impounds a reservoir (constant water depth), and the horizontal rigid rock. The hydrodynamic pressures are generated by horizontal motion of the dam semi-vertical US-face and by vertical motion of the horizontal reservoir bottom. Assuming water as linearly compressible and neglecting its internal viscosity and low amplitude, the irrotational motion of the water is governed by the wave equation. The normal pressure gradient of the hydrodynamic acoustic pressure $\Pi(x,y,z,t)$, at the vertical US-face of the dam, is proportional to the total acceleration of the boundary condition by (1). The used approach is the Eulerian method because in structures the variables are the displacements, while in fluids they are the pressures. In (1), ρ_w is the density of the water (the subscript w refers to the water); $\ddot{v}_g^n(t)$ is the ground acceleration in n-direction; $\varphi_1^n(\hat{n})$ is the component of the displacement in the dam 1st-mode natural vibration with an empty reservoir, and $\ddot{X}_1^n(t)$ is the modal coordinate that is associated to 1st-mode vibration. In (1), the second part represents the rigid pressures, whereas the third part represents the flexible pressure.

Considering only the vertically propagation waves due to the hydrodynamic pressure against the reservoir base, the boundary condition at the reservoir bottom is defined by (2). The fluid-foundation interaction has been shown in (2); where $\tilde{v}_{b,w}$ stands for the speed of water compressive wave, α_w is the wave reflection coefficient, $\mu = \rho_w/(\rho_f\ \tilde{v}_{b,f})$, $\tilde{v}_{b,f} = \sqrt{(E_f/\rho_f)}$, E_f is the Young's modulus of the foundation and ρ_f is the density of the foundation medium. For a rigid foundation $\tilde{v}_{b,f} = \infty$ and $\mu = 0$. Third term in (2) represents the modification of the vertical acceleration, i.e. $\ddot{v}_g^y(t)$ in the second term, which depends on the interaction between the fluid and flexible semi-infinite foundation. Since the pressure in the third term depends on the time t, the reservoir bottom produces a damping effect due to the radiated energy by means of the refraction of the waves in the foundation. The refracted waves can be dilatational (tensile or compressive deformations) and rotational (shear deformations). The other pressure waves are reflected in the water medium (in US-direction a part of the energy is lost). Since that the foundation is considered axially flexible with infinite length and infinitesimal width, only refracted waves are downward vertical waves. The hydrodynamic pressures have been calculated using $\alpha_w = 0.85$ that is the ratio of the amplitude of the reflected hydrodynamic wave and the amplitude of the vertical propagating wave incident on the bottom; it depends on the angle of incidence, sediment mass density, sound velocity in sediment, sediment layer depth and acoustic

impedance ($1/\mu$): dynamic stiffness between the layer of the reservoir and the layer of the rock (interface complex forces in the frequency domain between both layers). When $\alpha_w = 1$ ($\mu = 0$) the pressure has the same values of the hydrodynamic pressure for water compressible. When $\omega_{1,w} < 2\omega_{1,d}$ it is necessary an elaborated analysis of α_w. In this study $\omega_{1,w}/\omega_{1,d} = 0.8907$. For high dams a several analysis based on different values of the α_w is always required. For $\alpha_w = 0.85$ (i.e. the waves are mainly reflected in the water, 85%, and partially transmitted into the substrate, 15%) the maximum horizontal hydrodynamic pressure is 0.83 lesser than the maximum horizontal hydrodynamic pressure for $\alpha_w = 0.41$. Usually, it is possible to adopt $\alpha_w \approx 0.8$[15]. Neglecting the water superficial waves, the boundary condition at the free surface of the reservoir is: $\Pi(\hat{n},t) = 0$.

The hydrodynamic pressure satisfies the radiation condition in the US-direction (for infinity or semi-infinity length) by (3). The normal vector $\hat{n}$ refers, in all equations, to the interface of the considered boundary. To consider the ground acceleration in the circular frequency (ω) domain, the wave equation becomes the Helmholtz equation. When the interaction between the dam and the impounded water needs a solution in the frequency domain the water must be considered compressible. The described pressures are valid to calculate the excitation in the horizontal and vertical direction for rigid or flexible dams. In this study, only the effect due to the horizontal acceleration has been studied.

The foundation should be analyzed under the assumptions of anisotropy and nonlinear behavior for the rock, including the wave equations, but it is almost-impossible to take in account all rock discontinuities because geological data of the rock layers are not usually available. In the 3-D model the foundation can be defined by the rock and mass-less linear model.

Because of the complexity in the global analysis, divided substructure methods are preferred for the seismic analysis of dams. The three-system liquid-dam-rock can be divided in two parts: dam-foundation and dam-water. The equation of the motion for the dam-foundation system, in the *n*-direction, is[16]:

$$[M]\{\ddot{v}(t)\} + [C]\{\dot{v}(t)\} + [K]\{v(t)\} = -[M]\{\ddot{v}_g(t)\} + \{\Gamma(t)\} \tag{4}$$

in which M is the mass matrix, C is the damping matrix and K is the stiffness matrix. The displacement $v(t)$, velocity $\dot{v}(t)$ and acceleration $\ddot{v}(t)$ are the relative vectors to the soil base. The equation (4) represents the assembled system of two substructures where the foundation is idealized as a continuum. The first and second line of (4) are, respectively (the subscripts f refers to the foundation, whereas d refers to the dam):

$$m_d\ddot{v}_d(t) + (c_d + c_f)\dot{v}_d(t) - c_f\dot{v}_f(t) + (k_d + k_f)v_d(t) - k_f v_f(t) = -m_d\ddot{v}_g(t) \tag{5}$$

$$m_f\ddot{v}_f(t) - c_f\dot{v}_d(t) + c_f\dot{v}_f(t) - k_f v_d(t) + k_f v_f(t) = -m_f\ddot{v}_g(t) + \Gamma_f(t) \tag{6}$$

with $\Gamma_f(t) = c_{df}(\dot{v}_{df}(t) - \dot{v}_f(t)) + k_{df}(v_{df}(t) - v_f(t))$, which is the interaction force between dam-foundation. The equation of the motion for the dam-water (not matrix system) is:

$$m_d\ddot{v}_d(t) + c_d\dot{v}_d(t) + k_d v_d(t) = -m_d\ddot{v}_g(t) + \Phi_w(t) \tag{7}$$

where $\Phi_w(t)$ is the exerted nodal force on the wall due to the hydrodynamic pressure. It is possible to think this force as an "elastic" force of the dam-rock-water system:

$$\Phi_{dw}(t) \equiv m_{dw}\ddot{\Pi}_e(t) + c_{dw}\dot{\Pi}_e(t) \tag{8}$$

in which, in a system assembled of two substructures, idealizing the water as a continuum, is:

$$k_{dw}(v_{dw}(t) - v_w(t)) \equiv \Phi_w(t) + c_{dw}(\dot{v}_{dw}(t) - \dot{v}_w(t)) \tag{9}.$$

Equation (8) has been obtained from discretization of the wave equation[17] where $\Pi_e(t)$ is the nodal pressure vector. The introduction of this variable is more consistent to study the fluid behaviour: usually, the response of the fluids is measured in terms of velocity or pressure, not in terms of displacement as (9).

5 Non-linear Seismic Analysis

During the vibration, a part of energy is dissipated irreversibly via structural instability, plasticity and creep; whereas the other part of the energy is stored via elastic strain energy which can be reused by the structure. The structural mechanical properties change during the analysis; in this sense, the stiffness and strength have a systematically decrement. The used non-linear model is based on the combination of plasticity theory[18] and damage mechanism. The criteria are: (i) Modified Mohr-Coulomb[19] (MMC) yield criterion, (ii) associated flow rule and (iii) softening curve. Flow rule describes the increment of plastic strain and, when the concrete is subject to severe inelastic state, the plastic distortion changes the concrete volume. Flow rule is called "associated" when the plastic potential is equal to yield function. The MMC criterium determines the stress when yielding occurs and regards the total damage to be equal only to the cohesion. The evolution of the yield branch (softening) is controlled by the cohesion curve which justifies the MMC choice. MMC is a function of the uniaxial stress component and considers the isotropic homogeneous material. However, it is worth to note that the failure depends more on the heterogeneous behaviour of the material.

The Plastic-Damage (PD) model, taking into account the stiffness degradation, is more appropriate to analyze the crack and failure of the concrete arch dams. The plastic stiffness considers a single variable, i.e. the tensile damage factor d_t. It varies from 0 (undamaged elastic material) to 1 (fully damaged material)[6]. In this study we have also considered that, during the load cycles, the slope of the elastic modulus ($E_{d,ei}$) decreases, therefore reloading is simulated by non-parallel lines to the initial slope of $E_{d,e0}$ (initial elastic modulus). However, the elastic modulus is underestimated because the recovery during the unloading phase has not been considered. The plastic stiffness is defined by $E_{d,ei}(1 - d_t)(1 - d_c)$. The compression damage factor has been considered $d_c = 0$ because the focus of the current work is only to study the concrete tensile behaviour. These two variables, d_t and d_c, aim at two distinct phenomena (cracking and crushing) that usually occur in the concrete under cyclic loadings. In this study, four idealized hysteretic cycles step-by-step have been considered: $\{E_{d,ei} | \ i = 1,2,3,4\}$. The exponential and linear Tension Softening Curve (TSC) has been used (see Fig. 3 (left)). Table 5 shows the concrete parameters which are obtained from iterative analyses supported by literature[4,5,6,20].

Table 5 Concrete parameters.

Tensile strength (f_t) [MPa]	2.73
Compressive strength (f_c) [MPa]	47.5
Initial elastic modulus ($E_{d,e0}$) [GPa]	1.2 x 37 = 44.40 GPa[7,21]
Poisson's ratio of the dam (v_d)	0.19*
Tension specific fracture energy (G_t) [N/m]	113.06
Characteristic micro-crack openings that propagate through the aggregates (w_c) [μm]	240.51
Crack band width of the fracture (l_c) [m]	0.45
Size of the element which models l_c for the linear analysis (h_0) [m]	1.35
Effective crack length (a_c) [m]	0.484**
Limit dynamic tensile strain (ε_{lt}) [μm]	165.87**

*Poisson's ratio of the dam usually ranges 0.15-0.25.
**The effective crack length has been estimated using data from literature[22,23]. The limit dynamic tensile strain, in accordance to literature[1,15].

To define ε_{lt} the characteristic length is been assumed 0.50 m, which represents the side of an equivalent cube of the volume of the 3-D solid element[15]: it can be utilized to study the crack phenomenon using only the mesh in FEA.

Figure 3 (left) shows the exponential and linear (dashed line) TSC. The filled area is the G_t/1.354. The G_t has been increased by experimental value in literature as already mentioned. The area under the stress line overestimates the tension softening curve of 2.9. Figure 3 (middle) shows the blocks of the dam during construction.

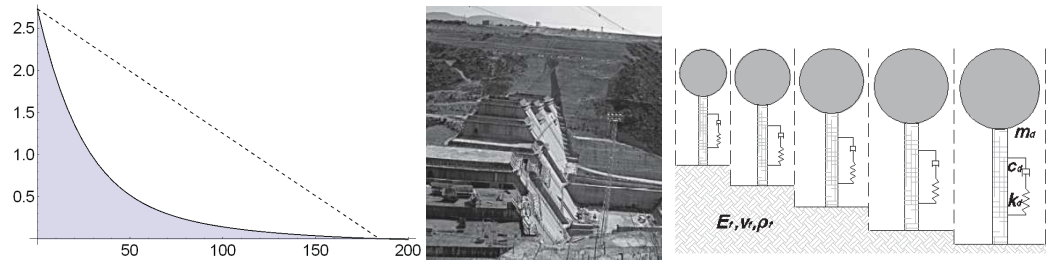

Fig. 3 Simple oscillators of the model by AutoCAD©software (from left to right: 14A, 12A, 10A, 8A, 0A) (right); blocks of the dam during construction (middle); exponential and linear TSC (left). TSC curves define the tensile strength (in MPa) vs. crack opening (μm) with the range 0-2.73 and 0-240.51, respectively.

In Fig. 3 (middle) it is possible to note that the blocks are constructed in different stage, changing the distribution of the stresses step-by-step. However, since the most important weight is the dead-weight, the construction in different stage does not influence much the final configuration of the stresses (except the variation of the temperature). In Fig. 3 (right) the oscillators of the five analyzed blocks and the matrix coefficients are shown – in (4) the matrix M, C and K are defined by matrix coefficients m, c and k, respectively. The oscillators are scaled each other in accordance to real height

(see Table 4): the relation between 14A and 0A (Fig. 3 (right)), is 1.679. The foundation rock parameters have also been shown: E_f = 41.55 GPa, ρ_f = 2.8 x 10^3 kg/m^3, v_f = 0.31 (Poisson's ratio of the foundation).

6 Results and Conclusions

Time-history (TH) continuum approach by Wolfram Mathematica has been made. Each block has been considered as a simple oscillator, therefore the relation, considering the displacement in the top, between the stiffness and modulus is known. The increase of the dynamic loads in respect to the static loads has been taken into account considering the increase of the stiffness. It is also possible, and more convenient, to consider this increasing by a dynamic magnification factor to the elastic modulus (e.g., see coefficient used to define $E_{d,e0}$ in the Table 5). Due to around 10 m of the dam being fixed in the foundation and the modal participating mass ratio for the first three modes in the three directions being 83.7%, the dynamic mass has been assumed 90% of the static mass. The used dam damping ξ_d is 5% and it is constant during the analysis. The foundation hysteretic damping is 10%. The system (dam-foundation-reservoir) damping is 8.5%. The equivalent stiffness is obtained from equivalent inertia (see Table 4), which depends on the mass. The participating mass of the dam fundamental mode in the three directions is 45.1%; from this value the estimated coefficient that reduces the inertia is 0.03182.

Figures 4–5 show linear and non-linear response. The suggested unacceptable ultimate displacements[24,25] v_{ult} are: 0.13 m, 0.12 m, 0.10 m, 0.09 m and 0.07 m for the blocks 0A, 8A, 10A, 12A and 14A, respectively. Consist to the literature[3,6], the acceptable elastic displacement is v_{el} = v_{ult}/4. Both displacements, v_{ult} and v_{el}, are indicated in Figs. 4–5 by horizontal dashed lines.

In Figs. 4–5, the gray filled area represents the disadvantage that the structure has in the plastic state. The portion of the gray filled area that exceeds v_{el} represents the permanent deformation, whereas the portion of the gray filled area that exceeds v_{ult} represents the damage.

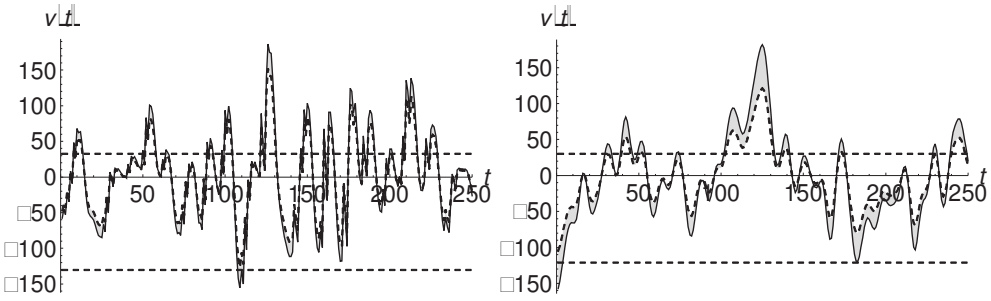

Fig. 4 Nonlinear and linear (dashed curve) TH analysis of the block 0A (left) and of the block 8A (right). The displacement is in mm.

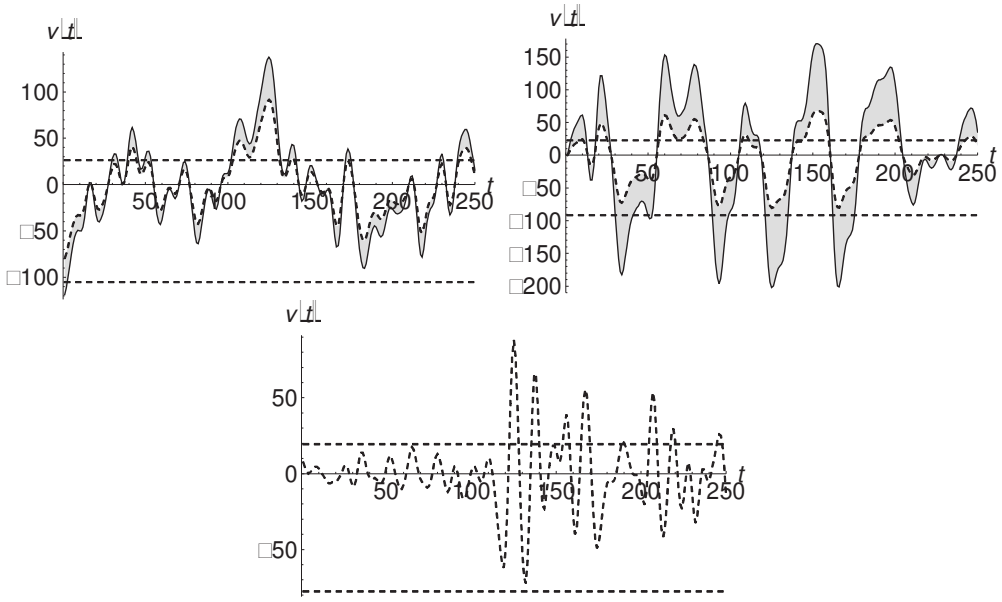

Fig. 5 Nonlinear and linear (dashed curve) TH analysis of the block 10A (left), 12A (right) and 14A (below). The displacement is in mm.

In the nonlinear analysis the gradually descending acceleration values have been considered, i.e. for the first cycle we use the acceleration with the higher value whereas for the fourth cycle we use the acceleration with the lower value. The idea is to simulate a strong earthquake and then three relevant after-shocks.

The hydrostatic and hydrodynamic forces have not been considered: they are about 2.49% and 0.52% of the pseudo-dynamic seismic force of the dam, respectively.

The seismic events described in previous section have been recorded by a number of seismic stations. The acceleration peaks in the TH analyses are: 346.28 cm/s^2 (Turkey, 1999), 242.83 cm/s^2 (Greece, 13/09/1986), 162.08 cm/s^2 (Italy, 29/05/2012) and 93.49 cm/s^2 (Italy, 26/09/1997). The difference between 346.28 cm/s^2 and the maximum value 5000 shown in Fig. 1 (right) is due to the fact that the values were recorded from different seismic stations.

The time scale in Figs. 4 and 5 is "virtual" since only a portion of 250 points with a time interval of 1.25 s ($\Delta t = 1.25/250 = 0.005$) of the four accelerograms have been taken. These intervals contain the four acceleration peaks. This interval comprises only a part of the complete TH, therefore some responses have a different initial drift. The axis of abscissa in Figs. 4 and 5 corresponds to the set: $\{v_i(t_j) \mid \forall v_i \in R, \forall t_j \in N, i \in R, j = (0,1,2,...,250)\}$.

In Table 6 the non-linear response of the five blocks is shown, where the $E_{d,ep}$ is the dam elasto-plastic modulus, $v_{el,max}$ and $v_{ep,max}$ are the maximum elastic displacement and maximum elasto-plastic displacement, respectively. The estimated greater unacceptable ultimate displacements[24,25] v_{ult} is 0.13 m. For displacements over 2 x 0.13 = 0.26 m = 260 mm, it has been considered that the structure might suffer severe damage (= sd).

Table 6 Non-linear analysis results. The displacement is in mm.

	$E_{d,ep}$ = 35.52 GPa		$E_{d,ep}$ = 20.25 GPa		$E_{d,ep}$ = 7.69 GPa		$E_{d,ep}$ = 1.46 GPa	
	$v_{el,\,max}$	$v_{ep,\,max}$	$v_{el,\,max}$	$v_{ep,\,max}$	$v_{el,\,max}$	$v_{ep,\,max}$	$v_{el,\,max}$	$v_{ep,\,max}$
0A	151.652	186.409	140.204	210.469	-163.666*	sd	sd	sd
8A	131.114	161.164	121.217	181.965	-141.501*	sd	sd	sd
10A	99.146	121.870	91.662	137.599	-107.001*	-268.461*	162.065	sd
12A	74.680	91.796	69.042	103.643	-80.596*	-202.212*	122.072	sd
14A	53.728	66.042	49.672	74.566	-57.984*	-145.408*	87.824	sd

*The absolute value must be considered. The negative values are consistent with the TH in Figs. 4 and 5.

In Table 7 working accumulation in terms of the displacement, v_{acc}, that exceeds v_{el} and v_{ult}, is shown. The former represents the accumulation of the plastic deformation and the latter represents the accumulation of the cracks. $\overline{x}$ is the mean value of the accumulation sums (amount of damage) of the considered cycle. The standard deviation σ is calculated by all the accumulations of the four cycles.

Finally the 3-D post-seismic analyses by FEA have been made considering the displacement due to hydrostatic actions for the full reservoir. Considering $E_{d,ep}$ = 1.46 GPa and v_c = 0.15 the maximum displacement in the DS direction of the whole dam is 67.179 mm. This displacement is not very large due to fact that the curvature of the arch dams produces greater stiffness (in the pre-seismic phase, the whole dam displacement is 13.77 mm).

Table 7 Non-linear accumulations of the displacements (in mm).

	v_{acc} {v_{el}} for $E_{d,ep}$ (GPa)				$\overline{x}$	σ	v_{acc} {v_{ult}} for $E_{d,ep}$ (GPa)
	35.52	20.25	7.69	1.46			20.25
0A	2043.514	4099.721	-	-	3071.617	±12.095	1002.972
8A	1723.265	3505.312	-	-	2614.288	±10.423	631.495
10A	1237.635	2542.294	16030.540	-	6603.490	±40.252	410.842
12A	905.991	1808.057	12023.073	-	4912.373	±30.590	166.170
14A	612.915	1171.511	8608.578	-	3464.334	±22.260	0

The decrease of the elastic-plastic modulus can be seen as an increase of the dam flexibility in terms of the vibration period (in 3-D analysis the reduction of vibration period is 4.93).

7 Acknowledgements

The first author acknowledges the Servicios Informáticos CPD of the University of Salamanca for the Mathematica software license. The third author acknowledges support by CNPq, a Brazilian research funding agency.

References

[1] Omidi, O. and Lofti, V., Seismic plastic-damage analysis of mass concrete blocks in arch dams including contraction and peripheral joints, *Soil Dynamics and Earthquake Engineering,* vol. 95, pp. 118–137, 2017.

[2] Zhang, Q. L., Wang, F., Gan, X. Q. and Li, B., A field investigation into penetration cracks close to dam-to-pier interfaces and numerical analysis, *Engineering Failure Analysis,* vol. 57, pp. 188–201, 2015.
[3] Alembagheri, M., Earthquake damage estimation of concrete gravity dams using linear analysis and empirical failure criteria, *Soil Dynamics and Earthquake Engineering,* vol. 90, pp. 327–339, 2016.
[4] Omidi, O., Lotfi, V. and Valliappan, S., Plastic-damage analysis of Koyna dam in different damping mechanisms with dam-water interaction, *15th World Conference on Earthquake Engineering, WCEE 2012,* Lisbon, Portugal, 24–28 September, 2012.
[5] Guanglun, W., Pekau, O. A., Chuhan, Z. and Shaomin, W., Seismic fracture analysis of concrete gravity dams based on nonlinear fracture mechanics, *Engineering Fracture Mechanics,* vol. 65, pp. 67–87, 2000.
[6] Wang, J. T., Jin, A. Y., Du, X. L. and Wu, M. X, Scatter of dynamic response and damage of an arch dam subjected to artificial earthquake accelerograms, *Soil Dynamics and Earthquake Engineering,* vol. 87, pp. 93–100, 2016.
[7] Zacchei, E., Molina, J. L. and L. R. F. Brasil, M. R., Seismic hazard assessment of arch dams via dynamic modelling: an application to the Rules Dam in Granada, SE Spain, *International Journal of Civil Engineering*, pp. 1–10, 2017.
[8] Sabetta, F. and Pugliese, A., Estimation of response spectra and simulation of nonstationary earthquake ground motions, *Bulletin of the Seismological Society of America,* vol. 86, pp. 337–352, 1996.
[9] Ambraseys, N. N., Simpson, K. A. and Bommer, J. J., Prediction of horizontal response spectra in Europe, *Earthquake Engineering and Structural Dynamics,* vol. 25, pp. 371–400, 1996.
[10] Ambraseys, N. N., Douglas, J., Sarma, S. K. and Smit, P. M., Equations for the estimation of strong ground motions from shallow crustal earthquakes using data from Europe and the Middle East: Horizontal peak ground acceleration and spectral acceleration, *Bulletin of Earthquake Engineering,* vol. 3, pp. 1–53, 2005.
[11] Gaspar-Escribano, J. M., Navarro, M., Benito, B., García-Jerez, A. and Vidal, F., From regional- to local-scale seismic hazard assessment: examples from Southern Spain, *Bulletin of Earthquake Engineering*, vol. 8, pp. 1547–1567, 2010.
[12] Benito, M. B., Navarro, M., Vidal, F., Gaspar-Escribano, J., García-Rodríguez, M. J. and Martínez-Solares, J. M., A new seismic hazard assessment in the region of Andalusia (Southern Spain), *Bulletin of Earthquake Engineering*, vol. 8, pp. 739–766, 2010.
[13] Fenves, G. and Chopra, A. K., Effects of reservoir bottom absorption on earthquake response of concrete gravity dams, *Earthquake Engineering and Structural Dynamics,* vol. 11, pp. 809–829, 1983.
[14] Demirel, E., Numerical simulation of earthquake excited dam-reservoirs with irregular geometries using an immersed boundary method, *Soil Dynamics and Earthquake Engineering,* vol. 73, pp. 80–90, 2015.
[15] Mirzabozorg, H., Varmazyari, M. and Ghaemian, M., Dam-reservoir-massed foundation system and travelling wave along reservoir bottom, *Soil Dynamics and Earthquake Engineering,* vol. 30, pp. 746–756, 2010.
[16] Chakrabarti, P. and Chopra, A. K., Earthquake analysis of gravity dams including hydrodynamic interaction, *Earthquake Engineering and Structural Dynamics,* vol. 2, pp. 143–160, 1973.

[17] Seyedpoor, S. M., Salajegheh, J. and Salajegheh, E., Shape optimal design of arch dams including dam-water-foundation rock interaction using a grading strategy and approximation concepts, *Applied Mathematical Modelling,* vol. 34, pp. 1149–1163, 2010.
[18] Lubliner, J., Oliver, J., Oller, S. and Oñate, E., A plastic-damage model for concrete, *International Journal of Solids and Structures,* vol. 25, pp. 299–326, 1989.
[19] Oñate, E., Oller, S., Oliver, J. and Lubliner, J., A constitutive model for cracking of concrete based on the incremental theory of plasticity, *Engineering Computations,* vol. 5, pp. 309–319, 1988.
[20] Chen, H. H. and Su, R. K. L., Tension softening curves of plain concrete, *Construction and Building Materials,* vol. 44, pp. 440–451, 2013.
[21] U. S. Army Corps of Engineers (USACE), *Arch dam design*, Manual No. 1110-2-2201, 1994.
[22] Guan, J., Li, Q., Wu, Z., Zhao, S., Dong, W. and Zhou, S., Minimum specimen size for fracture parameters of site-casting dam concrete, *Construction and Building Materials,* vol. 93, pp. 973–982, 2015.
[23] Li, Q., Guan, J., Wu, Z., Dong, W. and Zhou, S., Equivalent maturity for ambient temperature effect on fracture parameters of site-casting dam concrete, *Construction and Building Materials,* vol. 120, pp. 293–308, 2016.
[24] Hariri-Ardebili, M. A., Seyed-Kolbadi, S. M. and Kianoush, M. R., FEM-based parametric analysis of a typical gravity dam considering input excitation mechanism, *Soil Dynamics and Earthquake Engineering,* vol. 84, pp. 22–43, 2016.
[25] Hariri-Ardebili, M. A. and Saouma, V., Quantitative failure metric for gravity dams, *Earthquake Engineering and Structural Dynamics,* vol. 44, pp. 461–480, 2015.